The influence of Tropical Indian Ocean SST on the Indian summer monsoon

Annalisa Cherchi[1], Silvio Gualdi[1], Swadhin Behera[2], Jing Jia Luo[2], Sebastien Masson[2], Toshio Yamagata[3], and Antonio Navarra[1]

[1]Istituto Nazionale di Geofisica e Vulcanologia, Bologna, Italy
[2]Frontier Research Center for Global Change/JAMSTEC, Yokohama, Japan
[3]Department of Earth and Planetary Science, The University of Tokyo, Tokyo, Japan

Manuscript submitted to

Journal of Climate

March 31, 2006

[0]*Correspondence to:* Annalisa Cherchi
Istituto Nazionale di Geofisica e Vulcanologia
Via Creti,12
I-40128 Bologna, Italy
e-mail cherchi@bo.ingv.it
Phone +39 051 4151438
Fax +39 051 4151499

Abstract

The Indian Summer Monsoon (ISM) is one of the main components of the Asian summer monsoon. It is well known that one of the starting mechanisms of a summer monsoon is the thermal contrast between land and ocean and that sea surface temperature (SST) and moisture are crucial factors for its evolution and intensity. The Indian Ocean, therefore, may play a very important role in the generation and evolution of the ISM itself. A coupled general circulation model, implemented with a high resolution atmospheric component, appears to be able to simulate the Indian summer monsoon in a realistic way. In particular, the features of the simulated ISM variability are similar to the observations.

In this study, the relationships between ISM and Tropical Indian Ocean (TIO) SST anomalies are investigated, as well as the ability of the coupled model to capture those connections. The recent discovery of the Indian Ocean Dipole Mode (IODM) may suggest new perspectives in the relationship between ISM and TIO SST. A new statistical technique, the *Coupled Manifold*, is used to investigate the TIO SST variability and its relation with the Tropical Pacific Ocean (TPO). The analysis shows that the SST variability in the TIO contains a significant portion that is independent from the TPO variability. The same technique is used to estimate the amount of Indian rainfall variability that can be explained by the Tropical Indian Ocean SST. Indian Ocean SST anomalies are separated in a part remotely forced from the Tropical Pacific Ocean variability and a part independent from that. The relationships between the two SSTA components and the Indian monsoon variability are then investigated in detail.

1 Introduction

The Indian Summer Monsoon (ISM) is one of the main components of the large-scale Asian summer monsoon. It is regulated by the thermal contrast between land and ocean, the large availability of moisture from the Indian Ocean, the Earth's rotation and the radiation from the sun (Webster, 1987; Meehl, 1997). It is characterized by large precipitation over India from June to September (Parthasarathy et al., 1992). Additionally, the abundant rainfall of the Bay of Bengal is an important component of the Indian summer monsoon precipitation, as shown by Goswami et al. (1999).

Summer rainfall over India is recognized to be influenced by sea surface temperatures (SSTs). Since the 1970s, many observational studies (Shukla and Misra, 1977; Weare, 1979; Shukla, 1987; Joseph and Pillai, 1984; Rao and Goswami, 1988), as well as modeling studies (Shukla, 1975; Washington et al., 1977), focused on the relationship between Tropical Indian Ocean (TIO) SST and ISM. The role of the TIO SST as active or passive element for the ISM has been a controversial issue. Webster et al. (1998) argued that Tropical Indian Ocean SST may be considered as a passive element of the ISM system at interannual time scale. On the other hand, several modeling studies have shown that the Indian Ocean does significantly affect ISM rainfall (Yamazaki, 1988; Chandrasekar and Kitoh, 1998; Meehl and Arblaster, 2002), and that the annual cycle of SST in the Indian Ocean is crucial for a realistic simulation of the Indian summer monsoon (Shukla and Fennessy, 1994). At the same time, many observational studies found out that positive SST anomalies over the Arabian Sea during the spring preceding the monsoon season are precursors for above normal precipitation over India (Weare, 1979; Joseph and Pillai, 1984; Rao and Goswami, 1988; Yang and Lau, 1998; Clark et al., 2000). However, the links between ISM and Indian Ocean SSTs during boreal summer are, as yet, not well understood.

The influence of the Equatorial and Western Pacific sea surface temperature anomalies (SSTA) on the Indian monsoon precipitation has been extensively studied (e.g., Rasmusson and Carpenter, 1983; Shukla and Paolino, 1983; Webster and Yang, 1992; Ju and Slingo, 1995; Soman and Slingo, 1997; Webster et al., 1998; Navarra et al., 1999; Miyakoda et al., 1999; Lau and Nath, 2000; Kinter et al., 2002; Miyakoda et al., 2003).

The basic result found in those studies is that the Indian summer monsoon and El Niño Southern Oscillation (ENSO) are negatively correlated. Moreover, evidence of a decadal variability affecting this relationship has been found, as its amplitude has decreased during recent decades (Kumar et al., 1999). Lau and Nath (2000) provided a mechanism, also known as the atmospheric bridge, to explain the influence of the Tropical Pacific Ocean on the monsoon by means of a suppression of convection over the western part of the Walker circulation in correspondence of a warm ENSO event. Recently, Kinter et al. (2002) and Miyakoda et al. (2003) studied in detail the influence of ENSO on the monsoon and vice versa, concluding that the teleconnection from ENSO to the monsoon tends to occur throughout the troposphere, while the teleconnection from the monsoon to ENSO involves mechanisms confined to lower levels.

Recently, the discovery of the Indian Ocean Dipole Mode (IODM; Saji et al., 1999; Webster et al., 1999), as an important mode of variability of the Indian Ocean itself, suggested the possibility of interactions between this mode of variability and the ISM. Later studies found controversial results. Ashok et al. (2001) and Li et al. (2003) argued that positive IODM events enhance ISM rainfall. In particular, Ashok et al. (2001) argued that the IODM influences the meridional circulation cell over the Indian sector in summer. Li et al. (2003) found that a strong ISM seems to be able to damp the original IODM event. Other studies (Webster et al., 2002; Loschnigg et al., 2003; Meehl et al., 2003) suggested a connection between positive IODM events and dry conditions over the Indian subcontinent. Lately, results from model experiments have confirmed that positive (negative) Indian Ocean dipole events may reduce the influence of an El Niño (La Niña) event on the Indian monsoon (Ashok et al., 2004).

The objective of this work is to investigate the influence of the TIO SST anomalies on the Indian summer monsoon and its relation with the Tropical Indian Ocean Dipole (TIOD) mode. We have used a long integration obtained from a coupled general circulation model (CGCM), and the results have been compared with observations and reanalysis. The ability of the coupled model to reproduce the main features of the climate of the Indian Ocean region, such as for example the IODM, has been shown in Gualdi et al. (2003b). Here, we analyze the characteristics of the simulated ISM, focusing on the feedbacks with the Tropical Indian Ocean.

A new statistical technique, the *Coupled Manifold*, recently developed by Navarra and Tribbia (2005), is used to measure the fraction of Indian summer monsoon variability influenced by Tropical Indian Ocean SST anomalies. Furthermore, as a substantial portion of the variability of the Tropical Indian Ocean is known to be linked to the variability in the Tropical Pacific Ocean (e.g., Wallace et al., 1998; Saji et al., 1999), the coupled manifold is used to divide the variability of Tropical Indian Ocean SST into a part remotely forced from the Tropical Pacific Ocean and a part free from that variability. The influence of the two components (free and forced) of Tropical Indian Ocean SST anomalies on precipitation over India is detected and analyzed, using the coupled manifold technique, to quantify the impact of free and forced TIO variability on the monsoon. The components of the SST found are used to investigate the mechanisms involved in the relationship between the tropical Indian Ocean SST and ISM.

The work is organized as follows: section 2 describes the coupled GCM, the reanalysis and observational datasets used to evaluate the model, and it contains also a brief description of the *Coupled Manifold* technique. Section 3 describes the mean state of the Indian Ocean and of the Indian summer monsoon and their variability. Section 4 includes an explanation of the effects of the tropical Indian Ocean SSTA on precipitation over India. Section 5 describes the Tropical Indian Ocean variability free and forced from the Tropical Pacific Ocean. Finally, section 6 contains a summary and a discussion of the main results obtained from this study.

2 Model, data and methodology

2.1 The SINTEX-F coupled model

The modeling results used in this study are obtained from a long integration (100 years) performed with the SINTEX-F CGCM (Luo et al., 2005). SINTEX-F is an evolution of the SINTEX CGCM (Gualdi et al., 2003a; Guilyardi et al., 2003), which has been proved to simulate a realistic climatology and variability of the Indian Ocean region (Gualdi et al., 2003b; Fischer et al., 2005). The analysis of the basic state in the Tropics, as simulated by SINTEX, indicates that there is no trend in the SST (Gualdi et al., 2003a).

Many of the systematic errors of SINTEX are still present in SINTEX-F (Luo et al., 2005; Masson et al., 2005). In the Pacific Ocean the cold tongue regime extends too westward, in association of strong trade winds simulated in the Eastern Pacific Ocean that extend westward (Gualdi et al., 2003a; Guilyardi et al., 2003). Furthermore, the model, as many coupled models, features an unrealistic double ITCZ (Gualdi et al., 2003a). Finally, in the eastern Indian Ocean a strong wind-SST-thermocline feedback is simulated (Fischer et al., 2005).

The atmospheric component is the fourth generation of the ECHAM atmospheric model developed at the Max Planck Institute für Meteorologie in Hamburg (Roeckner et al., 1996). In particular, the model version used is ECHAM4.6, which is parallelized through the Message Passing Interface. The ECHAM model is a global spectral model with a Gaussian representation for the horizontal grid and sigma vertical levels. The version we have used has a horizontal resolution at T106 triangular truncation corresponding to a grid of about $1.125^\circ \times 1.125^\circ$ and 19 vertical levels. The physics of the model is described in detail in Roeckner et al. (1996). The model uses a semi-Lagrangian transport scheme for the advection of water vapour and cloud water (Rasch and Williamson, 1990). The parameterization of convection is based on the mass flux concept (Tiedtke, 1989), modified following Nordeng (1994). The Morcrette (1991) radiation scheme is used with the insertion of greenhouse gases and a revised parameterization for the water vapour and the optical properties of clouds. The vertical turbulent transfer of momentum, mass, water vapour and cloud water is based on the similarity theory of Monin-Obhukov (Louis, 1979). The effect of the orographically induced gravity waves on momentum is parameterized by a linear theory and dimensional considerations (Miller et al., 1989). The soil model parameterizes the content of heat and water in the soil, the continental snow depth and the heat of permanent ice over continents and seas (Dümenil and Todini, 1992). The vegetation effects are parameterized following Blondin (1989).

The oceanic component is the OPA8.2 (Ocèan Paralelisée) ocean general circulation model (OGCM) with the ORCA2 configuration (Madec et al., 1998). The grid has two poles, one in the Eurasian continent and the other in the North American continent, to avoid the singularity over the North Pole. The horizontal resolution is about $2^\circ \times 2^\circ$, with an increase of the meridional resolution to 0.5° around the Equator. In the vertical there

are 31 levels, with 10 in the upper 100 m. The physics of the model includes a free surface configuration (Roullet and Madec, 2000). Vertical eddy diffusivity and viscosity coefficients are calculated from a 1.5 order turbulent closure scheme (Blanke and Delecluse, 1993).

The ocean and atmosphere components exchange SST, surface momentum, heat and water fluxes every 2 hours. The coupling and the interpolation of the coupling fields is made through the OASIS2.4 coupler (Valcke et al., 2000). No flux corrections are applied to the coupled model, except for the sea ice cover that is relaxed to observed monthly climatology in the ocean model.

2.2 Description of the datasets used for comparison

The results of the coupled model simulation have been compared with analysis and observed data. The SST fields are the Hadley centre sea-Ice and Sea Surface Temperature (HadISST1.1; full details are provided by Rayner et al., 2000). The CRU TS 2.0 dataset (Mitchell et al., 2003) contains global land precipitation on a regular grid ($0.5^\circ \times 0.5^\circ$ deg) for the period 1901-2002. Wind fields are taken from the ERA40 Reanalysis, realized from 1958 to 2002 (for more details see the web site http://www.ecmwf.int/research/era). Global distribution of ocean temperature is taken from an ocean analysis for the period 1948-1999 (Masina et al., 2004). All the observations and reanalysis datasets refer to the 1958-2002 period for consistency with the ERA40 time record length. The CMAP (CPC Merged Analysis of Precipitation) dataset is used to compare the climatology of precipitation over India and the adjacent ocean with the coupled model results. The CMAP dataset contains global monthly precipitation obtained by merging gauge data and 5 kinds of satellite estimates. The values are distributed on global regular gridded fields (grid point $2.5^\circ \times 2.5^\circ$) and cover a time period from 1979 to 2002 (Xie and Arkin, 1997).

2.3 The *Coupled Manifold*

The coupled manifold is a method to analyze covariation between fields. It is described and discussed in detail by Navarra and Tribbia (2005). The Appendix A, at the end of this paper, offers a brief summary of the main concepts used in this study. As explained in the

Appendix, the coupled manifold method has been applied to the EOFs coefficients of the considered fields. The results discussed in sections 4 and 5 have been obtained applying a significance test in the computation of the coupled manifold. The details concerning the test are discussed in the Appendix as well.

3 Mean state and variability

The description of the mean state of the tropical Indian Ocean in the SINTEX coupled model has been widely discussed by Gualdi et al. (2003a,b), Guilyardi et al. (2003), Terray et al. (2005). In this section we will focus on the mean state of precipitation, SST and wind fields during the boreal summer and fall over India and in the surrounding ocean.

In the boreal summer the Indian Ocean warms up (fig. 1, panel a). At the beginning of the monsoon season, winds in the Tropical Indian Ocean change direction: a strong south-westerly flow develops at low levels, whereas at upper levels a strong easterly jet is present. Near the surface, wind maxima are in July-August (fig. 2, panel a). In correspondence with the beginning and intensification of the monsoon winds, surface water cools down and a sea surface temperature gradient forms near the coast of Africa (fig. 1, panel a). Lindzen and Nigam (1987) have shown that in the Tropics a temperature gradient in the ocean is able to induce winds. The winds enhance evaporation which in turn may induce an intensification of the temperature gradient, generating feedbacks between surface temperature, surface fluxes and winds. The cooling of the SST in the Arabian Sea is maintained by southwesterly winds that bring moisture from the ocean toward the Indian subcontinent, the Bay of Bengal and South China.

In the coupled model the Tropical Indian Ocean is characterized by warmer than observed temperatures (fig. 1, panels c and d). Unfortunately, the model is not able to accurately simulate the summer changes of SST and near surface winds in the Tropical Indian Ocean. In particular, the SST gradient in the Arabian Sea is weaker than observed (fig. 1, panel c) and the south-westerly flow that develops is less intense (fig. 2, panel c). The weakness of the surface winds seems to be related to the feeble temperature gradient in the Arabian Sea: generally, weaker winds may induce smaller latent heat release, preventing a temperature decrease. In the model, the availability of surface moisture in

the western Tropical Indian Ocean is larger than observed (not shown), but the low-level winds are weaker than observed; a possible consequence is a reduction in the moisture advected toward India.

An important feature of the ISM is rainfall over the Indian subcontinent: starting from the end of May/beginning of June strong precipitation develops in the western part of India moving eastwards. In July-August (fig. 2, panel a) the whole of India experiences heavy rainfall. Generally, large precipitation tends to occur in correspondence of large low-level convergence. In particular, in the Bay of Bengal convection is sustained by the large availability of moisture in conjunction with strong low-level convergence. During the summer monsoon season, abundant precipitation falls over the Indian subcontinent with the main peaks in the Western Ghats and the Bay of Bengal (fig. 2, panel a). Important convective centres can also be found in the Indian Ocean, particularly to the east of the basin south of Sumatra and south of the Equator around 70°E. The patterns of precipitation are realistically simulated by the coupled model (fig. 2), though the amount of model precipitation in the Western Ghats and in the Bay of Bengal is less than observed (fig. 2 , panel c, d). Over the ocean, abundant rainfall is positioned too westward and the peak of 10 mm/day at the Equator is not realistic, while in the eastern part of the basin the simulated precipitation is weaker than observed (fig. 2 , panel c). Similar errors in the Western Ghats and in the Bay of Bengal precipitation can be found in the Echam atmospheric model (Roeckner et al., 1996; Cherchi and Navarra, 2005). In the coupled model the latent heat flux released and the cloud cover are weaker than observed, particularly over India and the Bay of Bengal (not shown).

As the monsoon proceeds and intensifies the amount of moisture at the land surface decreases (not shown), the latent heat released increases and, as a consequence, the temperature at the surface tends to cool down. From September-October the monsoon enters in its demise phase. Most of the Tropical Indian Ocean reaches a temperature of about 27°.5-28° C and the SST gradient over the Arabian Sea is reduced (fig. 1, panel b). At the same time, winds decrease both at low (fig. 2, panel b) and upper levels, and the precipitation over India and the Tropical Indian Ocean progressively disappears. This phase of the phenomenon is reproduced by the coupled model even if SST in the TIO remains warmer than observed (fig. 1, panel d), and the precipitation decrease over India is slower

than observed (fig. 2, panel d). The biases of the model in the simulation of the boreal fall precipitation and winds may be included in the systematic errors of the model, as already shown by Terray et al. (2005).

The annual cycle of precipitation averaged over India (70°-90°E, 5°-30°N), computed for both model and observations (fig. 3, panel a), emphasizes the good agreement between model and observations during the starting phase of the monsoon, and the deficiency in the rainfall amount simulated by the model in June and July. Moreover, the model tends to delay the demise of the monsoon, as in August and September it simulates more rainfall than observed.

We conclude the description of the mean state of the Tropical Indian Ocean with the analysis of the vertical structure of the temperature in the ocean. Fig. 4 shows the equatorial section of temperatures in the Tropical Indian Ocean for the upper 350m. The left panels in the picture contain the profiles obtained from an ocean analysis averaged in July-September (JAS) and October-December (OND), the middle panels show the same averages computed for the coupled model results, while the right panels show the difference between model and analysis. The simulated temperature in the upper 90 m tends to be generally warmer than observed, especially in the western part of the basin. The largest bias of the coupled model occurs in the boreal fall (fig. 4, panel d) when the upper 150 m are warmer than observed in the west of the basin and colder than observed in the east. In the same period, the simulated 28° isotherm slope is not realistic. A known bias of the Echam model, when coupled, is the tendency to have a too strong wind-thermocline-SST feedback in the Eastern Indian Ocean (Fischer et al., 2005), and a possible consequence is the overestimation of the IODM-like variability.

Usually, the year to year variability of the monsoon is studied through precipitation and circulation indices. A simple index commonly used is the average of the JJA mean precipitation anomalies over India (70°-90°E, 5°-30°N), that is the same area considered for the figure 3. This index, that we indicate as IMR (Indian Monsoon Rainfall, as already done by Wang and Fan, 1999), is a generalization of the well known AIR index introduced by Parthasarathy et al.(1992) and widely used to represent the variability of the Indian summer monsoon. Wang et al. (2001), in an observational study, defined a dynamic index, the Indian Monsoon Index (IMI), as the difference of the summer mean zonal wind at 850

mb averaged in 40-80°E, 5-15°N and averaged in 70-90°E, 20-30°N. This dynamic index represents the dominant mode of variability over the Indian subcontinent (Wang et al., 2001). The annual cycle of the index for both model and observations (fig. 3, panel b) indicates that the seasonality is well captured by the model, even if the intensity in the model is slightly weaker than observed from June to August, and the main peak occurs in August rather than in July. Similar biases have been observed for the IMR index. In the model, IMI and IMR are significantly correlated (the correlation coefficient is 0.68), so both of them can be considered a good index of the Indian summer monsoon variability.

The interannual variability of the Tropical Indian Ocean is assessed by means of an EOF analysis of the monthly SST anomalies, obtained by subtracting the seasonal cycle, in the 40°-120°E, 20°S-25°N area. In the observations, the first EOF is a basin-wide mode (not shown) which explains almost 33% of the variability in the Tropical Indian Ocean. As it has already been found and discussed in a number of observational and model studies (e.g., Wallace et al., 1998; Saji et al., 1999), this mode represents the variability of the Tropical Indian Ocean associated to the variability in the Tropical Pacific Ocean. The second mode explains about 12% of the Tropical Indian Ocean variability and exhibits a spatial dipole structure between the eastern and western part of the basin. This structure has been recently associated with the so called Indian Ocean Dipole Mode (IODM, Saji et al., 1999; Webster et al., 1999). In the coupled model, the first mode is basin-wide, consistently with the observations, and the second is a dipole mode (not shown), but some differences are visible. Specifically, the second EOF of the simulated SST has a stronger than observed dipole structure, with the negative pole in the eastern part of the basin that extends westward. Besides, in the model, the percentages of explained variance of the first two SST modes are not well separated. The first mode explains about 23% of the total TIO variability, whereas the second mode explains about 19%.

4 Effects of Tropical Indian Ocean SSTA on the ISM

Once the skill of the coupled model to reproduce the mean state and variability of both the Indian Ocean and the Indian summer monsoon has been assessed, it is of interest to investigate in detail the connection between SST over the tropical Indian Ocean and

precipitation over India.

The monsoon indices introduced and described in the previous section are a representation of precipitation over India, as already explained. Composite maps of strong (index $>$ 1std) minus weak (index $<$ -1std) years according to those indices have been computed to analyze the spatial structure of surface fields, such as precipitation, winds and SST. A non-parametric significance test, based on the bootstrap procedure, using a resampling technique (Wilks, 1995), has been applied to the composites. The patterns of the composites produced using the two indices (IMR and IMI) are similar. Specifically, above normal precipitation over India is linked to above normal precipitation over Indonesia, just south of the Equator, and with below than normal precipitation in a band along the Pacific Ocean, between the Equator and 10°N (not shown). Negative anomalies of precipitation along the Eastern Equatorial Pacific Ocean are associated with a cooling of that area (fig. 5, panel a). In the coupled model this feature is represented, even if negative anomalies in the Equatorial Pacific Ocean extend westwards, probably as a consequence of the tendency of the model to reproduce a cold tongue regime that extends far in the West Pacific Ocean. In the Indian Ocean the negative anomalies over the Arabian Sea are well captured by the coupled model. The main bias is found south of the Equator, where the model shows a dipole structure that is not realistic (fig. 5, panel b). The dipole structure in the Tropical Indian Ocean in correspondence of strong and weak monsoon years reaches its maximum intensity during the monsoon season, and then tends to disappear (not shown). It is possible to see from fig. 5 that the model exhibits some problems in the representation of the relationship between TIO SST and ISM. The biases observed can be in part ascribed to the systematic errors of the model reported previously, like the westward extension of the cold tongue regime in the Pacific Ocean and the strong wind-thermocline-SST feedback in the eastern Indian Ocean.

Near the surface, enhanced convection over India implies enhanced westerly winds from the Indian Ocean towards the Indian subcontinent (fig. 6, panel a). In the coupled model this pattern is represented, even if near the coast of India this westerly flow is deflected southward toward the coast of Sumatra in an unrealistic way (fig. 6, panel b).

The ”forced manifold” of the summer mean SST anomalies in the Tropical Indian Ocean (40°-120°E,20°S-25°N) and the summer precipitation anomalies in India, for both

model and observations, is computed to measure the variance of precipitation in India induced by SST anomalies in the Tropical Indian Ocean. The upper panels of fig. 7 represent the ratio of the variance of the ”forced manifold” to the total variance, that is the percentage of variance of precipitation in India linked to the SST anomalies in the Tropical Indian Ocean. A significance test, as explained in the Appendix, is applied to the ”forced manifold” computed, and all the values shown are significant at 95%.

In the observations (fig. 7, panel a), the influence of the Tropical Indian Ocean SST on summer precipitation in India is localized mainly in the southern and in the eastern part of the subcontinent. In these regions, at least a third of the variance of the precipitation is induced by the variability of the SST in the surrounding ocean. In the coupled model (fig. 7, panel c), the areas where the percentages of variance of precipitation in India induced by SSTA in the TIO are higher than 20% (shaded areas in the picture) are localized in the north-western and south-eastern part of the subcontinent. In the computation of the ”forced manifold” it is possible to have a measure, which we indicate with C, of the connection between the fields considered. For these fields that index is 0.17 in the observations and it is 0.25 in the coupled model. A value of 1 indicates that the ”forced manifold” includes the entire variability (see Navarra and Tribbia, 2005), in this case a small part, less than one third, of the variability of precipitation in India is induced by SST anomalies in the TIO. In the coupled model the dependence of the boreal summer precipitation in India on the summer SST in the Tropical Indian Ocean is higher than in reality.

The analysis of the influence of SSTA onto precipitation anomalies, just described, may be reversed. The coupled manifold technique allows the computation of the percentage of variance of SST in the Tropical Indian Ocean linked to precipitation anomalies in India. The ratio of the variance of the ”forced manifold” to the total variance, that is the variance of SST in the Tropical Indian Ocean induced by precipitation anomalies in India, is represented in the lower panels of fig. 7. It is interesting to note that the percentages of variance of SST in the TIO induced by the variability of precipitation in India are of the same order, or even higher, of the percentages of variance of precipitation in India induced by SSTA in the TIO. In the observations, the areas with the higher variance are localized in the Arabian Sea, the Bay of Bengal and in the south-eastern Tropical Indian

Ocean off the coast of Sumatra (fig. 7, panel b). The pattern in the Arabian Sea seems to be linked to the feedback between precipitation, winds and SST that takes place in that area, in correspondence of the evolution of the monsoon (Yang and Lau, 1998; Clark et al., 2000). The higher variance near the coast of Sumatra suggests a link between SST in that region and precipitation over India. This connection may be explained by means of a local Hadley circulation in the monsoon domain, as discussed by Annamalai and Slingo (2001). In the coupled model (fig. 7, panel d), the pattern is different, except for a high variance in the Arabian Sea. In the model, the dynamics introduced is simpler than in reality, and the main mechanism involved in the Indian Ocean seems to be a dipole between the eastern and western part of the basin. This mechanism is part of the systematic errors of the model described by Fischer et al. (2005), who emphasized the easy feedback occurring in the eastern Indian Ocean between SST, winds and thermocline. In the last two pictures, the quantifications of the connection between SST and precipitation are C=0.22 for the observations and C=0.34 for the model.

The variability of the Indian Ocean, as previously discussed, is not independent from the variability of the Pacific Ocean, so the ”forced manifold” between the summer SST over the Tropical Indian Ocean and the summer SST over the Tropical Pacific Ocean is computed. Fig. 8 represents the ratio of the variance of the ”forced manifold” to the total variance, and indicates that SST over the Tropical Indian Ocean is substantially influenced by SST from the Tropical Pacific Ocean. All the values shown in the figure are significant at 95%. In this case the index which measures the connection between the fields considered is C=0.43 in the observations and C=0.45 in the coupled model, suggesting that almost half of the variability of the SST in the Tropical Indian Ocean is connected, possibly forced, by the Tropical Pacific Ocean SST variability. In the observations (fig. 8, panel a), the spatial distribution of the variance indicates that in the Equatorial Indian Ocean more than 50% of the variability is induced by the Tropical Pacific Ocean. The same happens in the coupled model (fig. 8, panel b), even if in this case the variance is slightly weaker. Those results indicate that the connection between ENSO and the Tropical Indian Ocean region is weaker than observed. This has been noted also by Terray et al. (2005) and they suggested that a possible cause may be the biases of the coupled model in the simulation of the basic state of the Pacific Ocean documented by Gualdi et al. (2003a)

and by Guilyardi et al. (2003).

The technique used allows the separation of the SST anomalies in the Tropical Indian Ocean in two parts: one whose variability is remotely forced by the Tropical Pacific Ocean, that we will indicate as ”forced” SST anomalies, and a part whose variability is free from the Tropical Pacific Ocean, that we will indicate as ”free” SST anomalies. When the SST in the Tropical Indian Ocean are separated, we are able to investigate how the possible influence of the TIO SST in the ISM is triggered by the TPO. To evaluate the impact that the TIO has on the summer monsoon when it is forced or free from the influence of the Pacific Ocean, we may compute the ”forced manifold” of precipitation in India with ”forced” and ”free” TIO SST. In the observations, the percentages of variance of precipitation linked to the SST in the TIO ”forced” and ”free” from the TPO are small (fig. 9, panels a and b). The coefficient C previously introduced is 0.09 in the first case and 0.06 in the second. The variance of precipitation in India is shared between the ”forced” and the ”free” SST components with slightly higher variance located in the north-eastern part of the subcontinent in the ”forced” case. Also in the coupled model the patterns of the percentages of variance of precipitation in India linked to the ”forced” and ”free” components of the SSTA in the TIO are small (fig. 9, panels c and d). For the model, C=0.10 in the ”forced” component case and C=0.13 in the ”free” component case.

5 Forced and free SST variability in the Tropical Indian Ocean

As discussed in the previous section, using the coupled manifold technique, the variability of the summer SST in the Tropical Indian Ocean has been separated in ”forced” and ”free” SST anomalies, where ”forced” and ”free” are referred to the influence from the Tropical Pacific Ocean.

We may then speculate on the mechanisms involved in the connection between TIO SST and monsoon. To this purpose, summer SSTA (total, ”forced” and ”free”) have been correlated with monsoon indices. The results for the dynamic index (IMI) and for the precipitation index (IMR) are similar for both model and observations, and only the results related to the correlation between SST and IMI are shown in fig. 10.

In the observations, the correlation of boreal summer SSTA with the monsoon is weak

(fig. 10, panel a). In the picture values significant at 95% are shaded. A significant negative correlation exists between monsoon indices and SST in the Arabian Sea, this negative correlation indicates that a cooling (warming) of the Arabian Sea occurs in correspondence of a strong (weak) Indian summer monsoon. When the same correlation is applied to the ”forced” and ”free” SST components (fig. 10, panels b and c) interesting features appear. A positive significant correlation exists between IMI and the ”forced” component of SSTA in the south-eastern Tropical Indian Ocean near the coast of Sumatra (fig. 10, panel b), which indicates that a warming (cooling) of this area is associated to a strong (weak) monsoon and that this is triggered by the Tropical Pacific Ocean. In the ”free” SSTA component case (fig. 10, panel c) significant negative correlations are localized in the Arabian Sea and in the Bay of Bengal. A strong (weak) monsoon is associated to a cooling (warming) of those basins when the TIO is free from the TPO influence. This feature may be associated to the known local effect of cooling of the adjacent seas when the monsoon is strong (Yang and Lau, 1998; Clark et al., 2000).

In the coupled model the main features described above are reproduced (fig. 10, panels d, e and f), at least in term of large-scale patterns. A significant negative correlation exists between the monsoon index and the summer total SSTA in the Arabian Sea. The ”forced” component of SSTA in the south-eastern Equatorial Indian Ocean warms in correspondence of a strong monsoon, while triggered by ENSO. The ”free” component of SSTA in the Arabian Sea is cold (warm) when the monsoon is strong (weak), as a consequence of a local effect independent from the forcing from the TPO. Differences are evident while analyzing the behaviour in the coupled model, in particular there is not a clear distinction between the ”forced” and the ”free” SST variability. In both cases, a strong dipole-like dynamics dominates in the Tropical Indian Ocean, and the reasons may be ascribed to the simpler dynamics represented in the coupled model with respect to the real world, and to the systematic errors of the model already mentioned: the weakness of the relationship between ENSO and the monsoon (Terray et al., 2005) and the bias in the eastern Indian Ocean, where the feedback between ocean and atmosphere is too strong (Fischer et al., 2005).

The separated components of the TIO SSTA are used to investigate the details of the variability of the TIO as forced or free from the influence of the TPO, and their relation-

ship with the ISM.

An EOF analysis is applied to the ”forced” and the ”free” SST anomalies, for both observations and model (fig. 11), to evaluate the variability of the TIO as forced or free from the TPO. The variability of the ”forced” SST in the observations (fig. 11, panel a) is dominated by a basin wide mode, which explains 62% of the total variance. This result is consistent with the discussion of section 3, where the dominant mode of variability of the Tropical Indian Ocean was ascribed to the influence of the variability of the Tropical Pacific Ocean. The second mode of variability of the ”forced” SST anomalies in the Tropical Indian Ocean (fig. 11, panel b) explains 18% of the variance and has a spatial dipole structure between the eastern and western part of the basin. The first mode of variability of the ”free” SST anomalies of the TIO (fig. 11, panel c) is again a dipole mode, which explains 39% of the variance. These results suggest that the component of the TIO variability which is free from the influence of the TPO is dominated by a dipole mode, with positive anomalies in the western part of the basin and negative anomalies in the eastern part. From this analysis we may speculate that the dipole mode in the TIO may be part of the free variability of the basin as well as the result of the forcing from the TPO.

The coupled model reveals a different variability structure, compared to the observations, in that the dominant modes of both ”forced” and ”free” SST variability feature a dipole-like structure. The first EOF of the ”forced” SST anomalies (fig. 11, panel d) explains 52% of the variance and has a weak dipole structure between eastern and western Indian Ocean. In the other two modes shown (fig. 11, panels e and f) the dipole structure is stronger, the second EOF of the ”forced” SST component explains 31% of the variance, while the first EOF of the ”free” component explains 28% of the variance. These results suggest that in the coupled model the Tropical Indian Ocean has a dominant mode of variability represented by a dipole either if it is free or forced from the influence of the Tropical Pacific Ocean. It is worthwhile to note that the dipole pattern obtained from the ”free” SST anomalies resembles the pattern obtained with the observations, while the dipole pattern of the ”forced” SST is somewhat different from that observed. These results may suggest that the free variability of the Tropical Indian Ocean is well reproduced by the coupled model, while a systematic error occurs in the simulation of the mechanisms

involved in the teleconnection between the Pacific and the Indian sectors, thus influencing the simulation of the ISM. This is consistent with the discussion made by Terray et al. (2005).

The results obtained with the EOF analysis seem to suggest that the Tropical Indian Ocean tends to have a dipole mode of variability that can be forced from the Tropical Pacific Ocean but that can also be generated without that influence. The principal components of the EOFs represented in fig. 11, for both observations and model, are then used to investigate the relationship between Indian Ocean dipole mode and ISM, correlating the PCs of ”forced” and ”free” SST components with the monsoon indices (table 1). As discussed in the introduction, the results from the literature about this topic are controversial. From the results of table 1 we may argue that the first principal component of the ”forced” SSTA for both observations and model is not correlated with the monsoon, indicating that the dominant mode of variability forced by the Tropical Pacific Ocean is not linked to the monsoon. In the observation case this corresponds to the fact that the basin wide mode of variability of the Indian Ocean forced by ENSO is not related to the monsoon.

On the contrary, the second PC of the ”forced” component, for both observations and model, is negatively correlated with monsoon indices. This might indicate that a positive (negative) dipole mode triggered by ENSO corresponds to a weak (strong) monsoon. Finally, from table 1 it is not possible to reach final conclusions about the connection between ”free” dipole mode variability and monsoon. In particular, in the observations the correlation is not significant, whereas in the coupled model it is positive. In the coupled model a dipole mode free from the variability of the tropical Pacific Ocean seems to correspond to a stronger monsoon. Anyway, we may not exclude that this result is a consequence of the systematic error of the model in the eastern equatorial Indian Ocean, where strong positive SST anomalies are associated to a strong monsoon (fig. 5, panel b).

ENSO may be not the only external forcing affecting the evolution of a dipole mode in the Tropical Indian Ocean. Recent studies suggest that different processes may trigger the IODM, as the local Hadley cell in the western Pacific and the associated convection over South China Sea and Maritime Continents (Kajikawa et al., 2003), or as the Southern Annular Mode (Lau and Nath, 2004). Indeed, further studies are still necessary to

investigate IODM, ISM, ENSO and all the external forcings which may influence their inter-connections.

6 Discussions and conclusions

In this study a coupled model has been used to investigate the influence of Tropical Indian Ocean SST anomalies on the ISM, comparing the results with observations and analysis datasets. As a first step, the skill of the model to simulate the mean climatology and variability of the ISM and Tropical Indian Ocean is assessed.

The mean ISM is reasonably well simulated by the coupled model both in terms of precipitation and circulation features. The coupled model is able to reproduce the starting phase of heavy rainfall in India and the associated inversion of surface winds. The simulated circulation features described in section 3 are realistic both in timing and intensity. The amount of simulated precipitation in India is underestimated, particularly in the Western Ghats and in the Bay of Bengal. The annual cycle of precipitation averaged in India computed for both model and observations shows that the model tends to delay both the peak of precipitation and the demise of the summer monsoon. The seasonal cycle of the SST in the Tropical Indian Ocean is realistic, although the model tends to have warmer temperatures than observed. In the subsurface, the isotherms slope in winter with a warm pool in the eastern part of the basin, while in summer they tend to flatten. Furthermore, in autumn the model is not able to properly simulate the slope of the isotherms in the upper ocean. The tendency of the model to keep such a thermal structure in the subsurface may induce the model to overestimate the dipole-like variability in the Tropical Indian Ocean.

The EOF analysis applied to the monthly SST anomalies shows that the coupled model is able to reproduce the first two modes of variability observed, but the variances explained by these two modes are not well separated.

Analogously, the composite analysis of summer SST for strong and weak monsoon years shows the tendency of the coupled model to develop a dipole-like variability in the TIO. During the monsoon season and just after it, negative anomalies develop in the western Indian Ocean, while positive anomalies appear in the east, in association with stronger easterly winds. In summer, negative SST anomalies over the Eastern Equatorial

Pacific Ocean are associated with strong monsoon conditions. This is a confirmation that the negative relation existing in summer between the monsoon and ENSO is captured by the model.

The *Coupled Manifold* technique (Navarra and Tribbia, 2005) has been applied to the summer SST in the Tropical Indian Ocean and precipitation over India in order to measure the variance of precipitation forced by the SST. The ratio of the variance of precipitation forced by Indian Ocean SST to the total variance shows that precipitation over India is slightly influenced by Tropical Indian Ocean SSTs. By means of the same technique, the variance of SST in the TIO influenced by precipitation in India is computed as well. The results show that in both cases the percentages of variance in the model and observations are of the same order. The main differences between model and observations are found in the spatial distribution of this variance, in particular in the observations higher values are found in the Arabian Sea and in the south-eastern Tropical Indian Ocean, near the coast of Sumatra. In the coupled model the pattern is dominated by two poles of higher variance located in the western and in the eastern part of the basin. This pattern seems to be a consequence of the systematic errors of the model and of the simpler dynamics involved in the model with respect to the real world.

The variability of the Tropical Indian Ocean is strongly influenced by the variability in the TPO, as it has been shown in a number of studies. The *Coupled Manifold* technique applied to SST anomalies in the TIO and SST anomalies in the TPO confirms this result and shows that in the coupled model this influence is weaker than observed.

The computation of the ”coupled manifold” permits to separate the SST anomalies in the TIO into a part whose variability is affected by the variability of the SST anomalies in the Tropical Pacific Ocean, and into a part whose variability is independent from the TPO. In this context, we indicate as ”forced” SST anomalies in the Tropical Indian Ocean the component that is influenced by the TPO, and as ”free” SST anomalies in the Tropical Indian Ocean the anomalies that are independent from the variability of the TPO. The method is then applied to precipitation in India and the ”forced” and ”free” SSTA components found. The main result is that the impact of ”forced” and ”free” SST on the variance of precipitation in India are of the same order. In the coupled model the intensities are weaker and this weakness may be ascribed to the well known weak relationship between

monsoon and ENSO simulated in the model. This result suggests that in the coupled model the teleconnection between the Tropical Pacific Ocean and the Indian Ocean sector is only roughly captured by the model, leading to deficiency in the representation of precipitation in India and, as a consequence, of the ISM. But it could also be an indication of an insufficient control of the Indian monsoon precipitation by the TIO.

Once the anomalies of the TIO have been separated into ”forced” and ”free” from the influence of the TPO, the components found have been correlated with the monsoon indices to study the possible mechanisms involved in the relationship between TIO SST and monsoon with or without the influence of ENSO. Total, ”forced” and ”free” SST anomalies have been correlated with IMI. In terms of large-scale patterns, it may be concluded that the results obtained from the coupled model are consistent with the observations. Anyway, it may not be neglected that the systematic errors of the models, such as the weakness of the relationship between ENSO and the monsoon and the strong feedback between ocean and atmosphere in the Tropical Eastern Indian Ocean, as well as a possible weaker dynamics represented in the coupled model with respect to the real world, seem to induce a dominant and strong dipole-like dynamics in the TIO.

The variability of the ”free” and ”forced” SST anomalies of the TIO have been analyzed in detail to better understand how the Tropical Pacific Ocean may influence the Tropical Indian Ocean. The EOF analysis applied to the ”free” and ”forced” components of the Tropical Indian Ocean SST shows that the first EOF of the forced SST is still basin-wide, consistently with the forcing of the Pacific Ocean on the Indian Ocean. On the other hand, the second EOF of the forced SST and the first EOF of the free SST have a dipole mode. So dipole patterns in the Indian Ocean may be explained as forced by the Pacific Ocean, but they can also be induced by the free variability of the Indian Ocean. In the model the dipole structure is dominant and the EOFs of the ”forced” and ”free” components of the Tropical Indian Ocean SSTs confirm this tendency.

The principal components of the ”free” and ”forced” TIO SSTA are used to investigate the relationship between ISM and the dipole-like structure in the TIO. The main result of this analysis is the existence of a negative correlation between the dipole-mode structure and the ISM when forced by the TPO, both in the observations and in the model. In the ”free” SST component case, the correlation in the observations is negative but not signif-

icant, in the model it is positive but we may not exclude that this may be a consequence of the bias of the model in the south-eastern Equatorial Indian Ocean.

The statistical analysis used allowed us to explore some aspects of the reciprocal influence between ISM variability and the TIO SST anomalies in boreal summer. However, from our results it is not possible to draw a definite conclusion about the passive or active role of the TIO SST in the ISM features.

The coupled model results are consistent with the observations but the main biases that arise from this study seem to indicate that the model is not able to capture in an exhaustive way the relationship between the Pacific and the Indian sectors. The mean state of the simulated Tropical Indian Ocean has characteristics that are typical of a permanent dipole structure, furthermore the dominant mode of variability of SST in the Tropical Indian Ocean, either forced or free from the Tropical Pacific Ocean, is a dipole between the eastern and the western part of the basin.

Acknowledgements. The authors thank the Italy-U.S. Cooperation Program in Climate Science and Technology and the European Community project ENSEMBLES, contract GOCE-CT-2003-505539 for the financial support. The experiment used for this study has been executed on the NEC SX-6 at INGV in Bologna, and authors are grateful to E. Scoccimarro and P.G. Fogli for the technical support given, and to S. Masina for the ocean analysis. A. Cherchi thanks A. Alessandri for useful discussion on statistical techniques and A. Bellucci for his comments. The authors thank the anonymous reviewers which suggestions greatly improved the original manuscript.

Appendix A The coupled manifold

The main assumption made in the coupled manifold approach (Navarra and Tribbia, 2005) is that two atmospheric fields (Z and S) may be linked by a linear relation. If the fields considered are at discrete times, their relation may be written in terms of data matrices, as

$$\mathbf{Z} = \mathbf{AS} \tag{A1}$$

where

$$\mathbf{Z} = [z(1), z(2), \ldots, z(n)] \tag{A2}$$

$$\mathbf{S} = [s(1), s(2), \ldots, s(n)] \tag{A3}$$

are data matrices expressing fields at fixed times, while **A** is the matrix which represents the linear relation. **Z** and **S** in general are supposed to be rectangular, with the number of rows different from the number of columns.

To solve equation A1 and find **A**, it is possible to set a simple minimization problem, that is

$$min \parallel \mathbf{Z} - \mathbf{AS} \parallel_F^2 \tag{A4}$$

where the norm is the "Frobenius norm", defined as

$$\parallel \mathbf{X} \parallel_F^2 = trace(\mathbf{X}\mathbf{X}^{'}) \tag{A5}$$

with the apex that indicates the transpose. The minimization problem introduced is a kind of least square problem, known as "Procrustes problem" (Richman and Vermette, 1993).

A solution of equation A4 may be written as

$$\mathbf{A} = \mathbf{Z}\mathbf{S}^{'}(\mathbf{S}\mathbf{S}^{'})^{-1} \tag{A6}$$

The solution A6 is exact only if $\mathbf{S}\mathbf{S}^{'}$ is of full rank, otherwise a minimization solution may be found using a pseudoinverse. The pseudoinverse used by the authors is the Penrose definition (Golub and van Loan, 1989), that is defined in terms of the eigenmodes u_i of $\mathbf{S}\mathbf{S}^{'}$ as:

$$(\mathbf{S}\mathbf{S}^{'})^{-1} = \sum_{i=1}^{K} u_i \lambda_i^{-1} u_i^{'} \tag{A7}$$

where the summation extends over all non-zero eigenvalues/eigenvectors of the matrix. In this way modes that do not contribute to the variance of **S** are excluded from the inverse.

The operator **A** represents the functional relation between the fields **Z** and **S**. The strength of the relation depends on the value of the minimum. If the minimum is zero, the solution is exact and the relation **A**, that links **Z** and **S**, is linear. If the minimum is not zero, then it is only a portion of the field **Z** variability that can be associated with the variability of **S**.

The problem A1 may be posed also in its "sister" form:

$$\mathbf{S} = \mathbf{B}\mathbf{Z} \tag{A8}$$

in which **S** is trying to be expressed in terms of **Z** and an analogous minimization solution is obtained as

$$\mathbf{B} = \mathbf{S}\mathbf{Z}^{'}(\mathbf{Z}\mathbf{Z}^{'})^{-1} \tag{A9}$$

A and **B** are now two operators that express the relation between **Z** and **S**, but they are not equivalent. To simplify the computation, the method described may be applied to the EOFs coefficients of **Z** and **S** fields: in this way the reduction of the mathematical dimension of the problem is quite significant. This approach has been used in the analysis we made, and table A1 collects the number of modes retained in the EOF exercise for each field analyzed in this study. The % of variance explained by those modes is also specified.

Before applying a significance test, the matrices **Z** and **S** have been scaled with $(\mathbf{S}\mathbf{S}^{'})^{-1/2}$. With that substitution, the new solution obtained for **A** (and **B**) contains correlation coefficients which have been tested with a significance test based on the Student distribution. The T-test used has n-2 degrees of freedom and the confidence bounds are on an asymptotic normal distribution of $0.5log\frac{1+r}{1-r}$, with an approximate variance equal to $\frac{1}{n-3}$ (Fisher-z-transform method). The test described is applied to the coefficients of the matrix considered, and if they do not fit the confidence intervals they are put equal to zero, in this way only the values that are significant according to the level chosen (in our case 5%) are shown in the figures.

The method described may identify both one-way and two-way relations between fields. In the first case we end up with ”forced manifold”, in the second with ”coupled manifold”.

References

Annamalai, H., and J.M. Slingo, 2001: Active/break cycles: diagnosis of the intraseasonal variability of the Asian summer monsoon. *Clim. Dyn.*, **18**, 85–102.

Ashok, K., Z. Guan, N.H. Saji and T. Yamagata, 2004: Individual and combined influences of ENSO and the Indian Ocean Dipole on the Indian summer monsoon. *J. Climate*, **17**, 3141–3155.

Ashok, K., Z. Guan and T. Yamagata, 2001: Impact of the Indian Ocean Dipole on the relationship between the Indian monsoon rainfall and ENSO. *Geophys. Res. Lett*, **28**(23), 4499–4502.

Blanke, B., and P. Delecluse, 1993: Low frequency variability of the tropical Atlantic ocean simulated by a General Circulation Model with mixed-layer physics. *J. Phys. Oceanogr.*, **23**, 1363–1388.

Blondin, C., 1989: Research on land surface parameterization schemes at ECMWF. Proceeding of the Workshop on "*Parameterization of fluxes over land surface*", ECMWF, Reading, UK.

Clark, C.O., J.E. Cole and P.J. Webster, 2000: Indian Ocean SST and Indian summer monsoon rainfall: Predictive relationships and their decadal variability. *J. Climate*, **13**, 2503–2519.

Chandrasekar, A. and A. Kitoh, 1998: Impact of localized sea surface temperature anomalies over the equatorial Indian Ocean on the Indian summer monsoon. *J. Meteorol. Soc. Japan*, **76**, 841–853.

Cherchi, A., and A. Navarra, 2005: Sensitivity of the Asian summer monsoon to the horizontal resolution: Differences between AMIP-type and coupled model experiments. *Submitted on Climate Dynamics*.

Dümenil, L., and E. Todini, 1992: A rainfall-runoff scheme for use in the Hamburg climate model. In: *Advances in Theoretical Hydrology. A tribute to James Dooge* (J.P. O'Kane Ed.); European Geophysical Society Series on Hydrological Sciences, **1**, Elsevier Press, Amsterdam, 129–157.

Fischer, A.S., P. Terray, E. Guilyardi, S. Gualdi and P. Delecluse, 2005: Two independent triggers for the Indian Ocean Dipole/Zonal Mode in a coupled GCM. *J. Climate*, **18**, 3428–3449.

Golub, G.H., and C.F. van Loan, 1989: *Matrix computations*, 2^{nd} Ed., John Hopkins University Press, 642 pp.

Goswami, B.N., V. Krishnamurthy and H. Annamalai, 1999: A broad scale circulation index for the interannual variability of the Indian summer monsoon. *Quart. J. Roy. Meteor. Soc.*, **125**, 611–633.

Gualdi, S., A. Navarra, E. Guilyardi and P. Delecluse, 2003a: Assessment of the tropical Indo-

Pacific climate in the SINTEX CGCM. *Ann. Geophys.*, **46**, 1–26.

Gualdi, S., E. Guilyardi, A. Navarra, S. Masina and P. Delecluse, 2003b: The interannual variability in the Tropical Indian Ocean as simulated by a CGCM. *Clim. Dyn.*, **20**, 567–582.

Guilyardi, E., P. Delecluse, S. Gualdi and A. Navarra, 2003: Mechanisms for ENSO phase change in a coupled GCM. *J. Climate*, **16**, 1141–1158.

Joseph, P.V., and P.V. Pillai, 1984: Air-sea interaction on a seasonal scale over north Indian Ocean. Part I: Interannual variations of sea surface temperature and Indian summer monsoon rainfall. *Mausam*, **35**, 323–330.

Ju, J., and J. Slingo, 1995: The Asian summer monsoon and ENSO. *Quart. J. Roy. Meteor. Soc.*, **121**, 1133-1168.

Kajikawa, Y., T. Yasunari and R. Kawamura, 2003: The role of the local Hadley circulation over the western Pacific on the zonally asymmetric anomalies over the Indian Ocean. *J. Meteorol. Soc. Japan*, **81**(2), 259–276.

Kinter III, J.L., K. Miyakoda and S. Yang, 2002: Recent changes in the connection from the Asian monsoon to ENSO. *J. Climate*, **15**, 1203–1215.

Kumar, K.K., B. Rajagopalan and M.A. Cane, 1999: On the weakening relationship between the Indian monsoon and ENSO. *Science*, **284**, 2156–2159.

Lau, N.-C., and M.J. Nath, 2004: Coupled GCM simulation of atmosphere-ocean variability associated with zonally asymmetric SST changes in the Tropical Indian Ocean. *J. Climate*, **17**(2), 245–265.

Lau, N.-C., and M.J. Nath, 2000: Impact of ENSO on the variability of the Asian-Australian monsoons as simulated in GCM experiments. *J. Climate*, **13**, 4287–4309.

Li, T., B. Wang, C.P. Chang and Y.S. Zhang, 2003: A theory for the Indian Ocean Dipole-Zonal Mode. *J. Atmos. Sci.*, **60**, 2119–2135.

Lindzen, R.S., and S. Nigam, 1987: On the role of sea surface temperature gradients in forcing low-level winds and convergence in the Tropics. *J. Atmos. Sci.*, **44**(17), 2418–2436.

Loschnigg, J., G.A. Meehl, J.M. Arblaster, G.P Compo and P.J. Webster, 2003: The Asian monsoon, the tropospheric biennial oscillation, and the Indian Ocean Dipole in the NCAR CSM. *J. Climate*, **16**, 1617–1642.

Louis, J.F., 1979: A parametric model of vertical eddy fluxes in the atmosphere. *Bound.-Layer Meteorol.*, **17**, 187–202.

Luo, J.-J., S. Masson, E. Roeckner, G. Madec and T. Yamagata, 2005: Reducing climatology bias in an ocean-atmosphere CGCM with improved coupling physics. *J. Climate*, **18**(13), 2344–

2360.

Madec, G., P. Delecluse, M. Imbard and C. Levy, 1998: OPA version 8.1 Ocean General Circulation Model reference manual. *Technical report*, LODYC/IPSL Note 11.

Masina S., P. Di Pietro and A. Navarra, 2004: Interannual-to-decadal variability of the North Atlantic from an ocean data assimilation system. *Clim. Dyn.*, **23**, 531–546.

Masson, S., J.J. Luo, G. Madec, J. Vialard, F. Durand, S. Gualdi, E. Guilyardi, S. Behera, P. Delecluse, A. Navarra and T. Yamagata, 2005: Impact of the barrier layer on winter-spring variability of the South-Eastern Arabian Sea. *Geophys. Res. Lett.*, **32**, L07703, doi:10.1029/2004GL021980.

Meehl, G.A., 1997: The south Asian monsoon and the tropospheric biennial oscillation. *J. Climate*, **10**, 1921–1943.

Meehl, G.A., J.M. Arblaster and J. Loschnigg, 2003: Coupled ocean-atmosphere dynamical processes in the Tropical Indian and Pacific Oceans and the TBO. *J. Climate*, **16**, 2138–2158.

Meehl, G.A., and J. Arblaster, 2002: Indian monsoon GCM sensitivity experiments testing tropospheric biennial oscillation transition conditions. *J. Climate*, **15**, 923–944.

Miller, M.J., T.N. Palmer and R. Swinbank, 1989: Parameterization and influence of sub-grid scale orography in general circulation and numerical weather prediction models. *Meteor. Atmos. Phys.*, **40**, 84–109.

Mitchell, T.D., T.R. Carter, P.D. Jones, M. Hulme and M. New, 2003: A comprehensive set of high-resolution grids of monthly climate for Europe and the globe: the observed record (1901-2000) and 16 scenarios (2001-2100). *Submitted on J. Climate*.

Miyakoda, K., J.L. Kinter III and S. Yang, 2003: The role of ENSO in the South Asian monsoon and pre-monsoon signals over the Tibetan Plateau. *J. Meteorol. Soc. Japan*, **81**(5), 1015–1039.

Miyakoda, K., A. Navarra and M.N. Ward, 1999: Tropical-wide teleconnection and oscillation. II: The ENSO-monsoon system. *Quart. J. Roy. Meteorol. Soc.*, **125**, 2937–2963.

Morcrette, J.J., 1991: Radiation and cloud radiative properties in the European Center for Medium Range Weather Forecast forecasting system. *J. Geophys. Res.*, **96**, 9121–9132.

Navarra, A., and J. Tribbia, 2005: The coupled manifold. *J. Atmos. Sci.*, **62**(3), 310–330.

Navarra, A., M.N. Ward and K. Miyakoda, 1999: Tropical-wide teleconnection and oscillation. I: Teleconnection indices and type I/type II states. *Quart. J. Roy. Meteor. Soc.*, **125**, 2909–2935.

Nordeng, T.E., 1994: Extended versions of the convective parameterization scheme at ECMWF and their impact on the mean and transient activity of the model in the tropics. *Technical Memorandum 206*, ECMWF Research Department, European Center for Medium Range Weather

Forecasts, Reading, UK.

Parthasarathy, B., A.A. Munot and D.R. Kothwale, 1992: Indian summer monsoon rainfall indices: 1871–1990. *Meteorol. Mag.*, **121**, 174–186.

Rao, K.G., and B.N. Goswami, 1988: Interannual variations of sea surface temperature over the Arabian Sea and the Indian monsoon: A new perspective. *Mon. Wea. Rev.*, **116**, 558–568.

Rasch, P.J., and D.L. Williamson, 1990: Computational aspects of moisture transport in global models of the atmosphere. *Quart. J. Roy. Meteor. Soc.*, **116**, 1071–1090.

Rasmusson, E.M., and T.H. Carpenter, 1983: The relationship between the eastern Pacific sea surface temperature and rainfall over India and Sri Lanka. *Mon. Wea. Rev.*, **111**, 517–528.

Rayner, N.A., D.E. Parker, E.B. Horton, C.K. Folland, L.V. Alexander and P. Frich, 2000: The HadISST1 Global Sea-Ice and Sea Surface Temperature Dataset, 1871–1999. *Hadley Center Technical Note 17*.

Richman, M.B., and S.J. Vermette, 1993: The use of Procrastes target analysis to discriminate dominant source regions of fine sulfur in the western USA. *Atmos. Environ.*, **27A**, 475–481.

Roeckner, E., K. Arpe, L. Bengtsson, M. Christoph, M. Claussen, L. Dümenil, M. Esch, M. Giorgetta, U. Schlese and U. Schulzweida, 1996: The Atmospheric general circulation Model ECHAM4: Model description and simulation of present-day climate: *Max-Planck Institut für Meteorologie*, Report no. 218, Hamburg, 86 pp.

Roullet, G., and G. Madec, 2000: Salt conservation, free surface and varying volume: A new formulation for oceans GCMs. *J. Geophys. Res.*, **105**, 23 927–23 942.

Saji, N.H., B.N. Goswami, P.N. Vinaychandran and T. Yamagata, 1999: A dipole mode in the Tropical Indian Ocean. *Nature*, **401**, 360-363.

Shukla, J., 1987: Interannual variability of monsoons. *Monsoons*, J.S. Fein and P.L. Stephens Eds., Wiley Interscience, 399–464.

Shukla, J., 1975: Effect of Arabian sea-surface temperature anomaly on Indian summer monsoon: A numerical experiment with the GFDL model. *J. Atmos. Sci*, **32**, 503–511.

Shukla, J., and M.J. Fennessy, 1994: Simulation and predictability of monsoons; in *Proceedings of the International Conference on Monsoon Variability and Prediction*, Tech. Rep. WCRP-84, World Climate Research Program, Geneva, Switzerland.

Shukla, J. and M. Misra, 1977: Relationship between sea surface temperature and wind speed over the central Arabian Sea, and monsoon rainfall over India. *Mon. Wea. Rev.*, **105**, 998–1002.

Shukla, J., and D.A. Paolino, 1983: The Southern Oscillation and long range forecasting of the summer monsoon rainfall over India. *Mon. Wea. Rev.*, **111**, 1830–1837.

Soman, M.K., and J. Slingo, 1997: Sensitivity of the Asian summer monsoon to aspects of sea surface temperature anomalies in the Tropical Pacific Ocean. *Quart. J. Roy. Meteor. Soc*, **123**, 309–336.

Terray, P., E. Guilyardi, A.S. Fischer and P. Delecluse, 2005: Dynamics of the Indian monsoon and ENSO relationships in the SINTEX global coupled model. *Clim. Dyn.*, **24**, 145–168.

Tiedtke, M., 1989: A comprehensive mass flux scheme for cumulus parameterization in large-scale models. *Mon. Wea. Rev.*, **117**, 1779–1800.

Valcke, S., L. Terray and A. Piacentini, 2000: The Oasis coupler user guide version 2.4. *Technical report*, TR/CMGC/00-10, CERFACS.

Wallace, J.M., E.M. Rasmusson, T.P. Mitchell, V.E. Kousky, E.S. Sarachik and H. von Storch, 1998: On the structure and evolution of ENSO-related climate variability in the tropical Pacific: Lessons. *J. Geophys. Res.*, **103**(C7), 14 241–14 260.

Wang, B., R. Wu and K.-M. Lau, 2001: Interannual variability of the Asian summer monsoon: contrasts between the Indian and the Western North Pacific-East Asian monsoons. *J. Climate*, **14**, 4073–4090.

Wang, B., and Z. Fan, 1999: Choice of South Asian summer monsoon indices. *Bull. Am. Meteor. Soc.*, **80**(4), 629–638.

Washington, W.M., R.M. Chervin and G.V. Rao, 1977: Effects of a variety of Indian Ocean surface temperature anomaly patterns on the summer monsoon circulation: Experiments with the NCAR general circulation model. *Pure Appl. Geophys.*, **115**, 1335–1356.

Weare, B.C., 1979: A statistical study of the relationship between ocean surface temperatures and the Indian monsoon. *J. Atmos. Sci.*, **36**, 2279–2291.

Webster, P.J., 1987: The elementary monsoon. In: *Monsoons* (J.S. Fein and P.L. Stephens Eds.), Wiley-Interscience.

Webster, P.J., and S. Yang, 1992: Monsoon and ENSO: Selectively interactive systems. *Quart. J. Roy. Meteor. Soc.*, **118**, 877–926.

Webster P.J., C. Clark, C. Cherikova, J. Fasullo, W. Han, J. Loschnigg, and K. Sahami, 2002: "The monsoon as a self-regulating coupled ocean-atmosphere system". Meteorology at the Millenium. Academic Press, 198–219.

Webster, P.J., A.M. Moore, J.P. Loschnigg and R.R. Leben, 1999: Coupled ocean-atmosphere dynamics in the Indian Ocean during 1997-1998. *Nature*, **401**, 356–360.

Webster, P.J., V.O. Magana, T.N. Palmer, J. Shukla, R.A. Tomas, M. Yanai and T. Yasunari, 1998: Monsoons: Precesses, predictability and the prospects for prediction. *J. Geophys. Res.*,

103(C7), 14 451– 14 510.

Wilks, D.S., 1995: Statistical methods in the atmospheric sciences. Academic Press.

Xie, P., and P. Arkin, 1997: Global precipitation: A 17-year monthly analysis based on gauge observations, satellite estimates, and numerical model outputs. *Bull. Am. Meteor. Soc.*, **78**, 2539–2558.

Yamazaki, K., 1988: Influence of sea surface temperature anomalies over the Indian Ocean and Pacific Ocean on the tropical atmospheric circulation: A numerical experiment. *J. Meteorol. Soc. Japan*, **66**, 797–806.

Yang, S., and K.-M. Lau, 1998: Influences of sea surface temperatures and ground wetness on the Asian summer monsoon. *J. Climate*, **11**, 3230–3246.

Tables

Table 1. Linear correlation coefficients of IMI with ”forced” and ”free” PCs for both observations and model. One asterisk indicates values significant at 90%, while double asterisk indicates values significant at 95%

	PC1 forced	PC2 forced	PC1 free
Obs	-	-0.25*	-0.21
Model	-	-0.49**	0.24**

Table A1. Number of modes (explaining 90% of the variance) retained for each fields involved in the computation of the coupled manifold. ”IndiaTPREP” stands for total precipitation over India (70-90E, 5-30N), ”TrIndOcSST” stands for SST in the Tropical Indian Ocean (40-120E, 20S-25S), and ”TrPacOcSST” stands for SST in the Tropical Pacific Ocean (120E-90W, 30S-30N).

	IndiaTPREP	TrIndOcSST	TrPacOcSST
Obs	26	13	17
Model	44	17	26

Figure Captions

Fig. 1. Climatology of SST (deg C) averaged in July-August and in September-October for the HadISST dataset (panels a and b, respectively), and for the coupled model results (panels c and d, respectively). The contour interval is 0.5°C.

Fig. 2. Climatology of total precipitation (mm/day, contour lines) and of wind (m/sec, vectors) at 850 mb averaged in July-August and September-October for the CMAP dataset combined with ERA40 winds (panels a and b, respectively) and for the coupled model results (panels c and d, respectively). Contour intervals are 4,6,8,10 and 14 mm/day.

Fig. 3. Annual cycle of precipitation averaged over India (70-90°E, 5-30°N) for the observations (CRU dataset) and the coupled model results (panel a, lines with open and closed circles respectively) and annual cycle of IMI circulation index (see text for explanation) computed with zonal wind from the observations and from the coupled model results (panel b, lines with open and closed circles respectively).

Fig. 4. Equatorial sections of temperatures in the Tropical Indian Ocean averaged in JAS and OND for the analysis (panels a and b) and for the coupled model experiment (panels c and d). Contour interval is 2°, and the thicker line correspond to the 20° isotherm. Panels e and f show the differences of the model minus the analysis temperatures for the same seasons. Contour intervals are -2 -1.5 -1. -0.5 0 0.5 1 1.5 2 2.5 3, and the thicker line correspond to the 0 contour line.

Fig. 5. Composites of JJA SST anomalies (C deg) for the observations (panel a) and for the coupled model results (panel b). Strong minus weak monsoon years according to IMI index are chosen. Values shaded are significant at 95%.

Fig. 6. Composites of JJA wind anomalies at 850 mb (m/sec) for the observations (panel a) and for the coupled model results (panel b). Strong minus weak monsoon years according to IMI index are chosen. Values shaded are significant at 95%.

Fig. 7. Ratio of the ”forced manifold” variance to the total variance for summer precipitation in India (70-90°E, 5-30°N) (upper panels) and for the the summer SST anomalies in the Tropical Indian Ocean (40-120°E, 20°S-25°N) (bottom panels) for the observations (CRU vs HadISST, panels a and b, respectively) and for the coupled model results (panels c and d, respectively). Values shaded are higher than 0.2. All the values shown are significant at 95%.

Fig. 8. Ratio of the ”forced manifold” variance to the total variance for summer SST anomalies in the Tropical Indian Ocean (40-120°E, 20°S-25°N) linked to SST anomalies in the Tropical Pacific Ocean (120°E-90°W, 30°S-30°N) for the observations (HadISST dataset, panel a) and for the coupled model results (panel b). Values shaded are higher than 0.4. Only values significant at 95% are shown.

Fig. 9. Ratio of the ”forced manifold” variance to the total variance of summer precipitation in India with ”forced” and ”free” SST anomalies in the Tropical Indian Ocean for the observations (panels a and b, respectively) and for the coupled model results (panels c and d, respectively). ”Forced” and ”free” are referred to the influence from the Tropical Pacific Ocean. Only the values significant at 95% are shown.

Fig. 10. Correlation coefficients between IMI and total, ”forced” and ”free” SST anomalies in the TIO for the HadISST dataset (panels a, b and c, respectively) and for the coupled model results (panels d, e and f, respectively). Values shaded are significant at 95%.

Fig. 11. First and second EOFs of the ”forced” Tropical Indian Ocean SST anomalies for the HadISST dataset (panels a and b, respectively) and for the coupled model results (panels d and e). First EOF of the ”free” Tropical Indian Ocean SST anomalies in the HadISST dataset (panel c) and in the coupled model results (panel f). ”Forced” and ”free” refers to the influence from the Tropical Pacific Ocean.

Figures

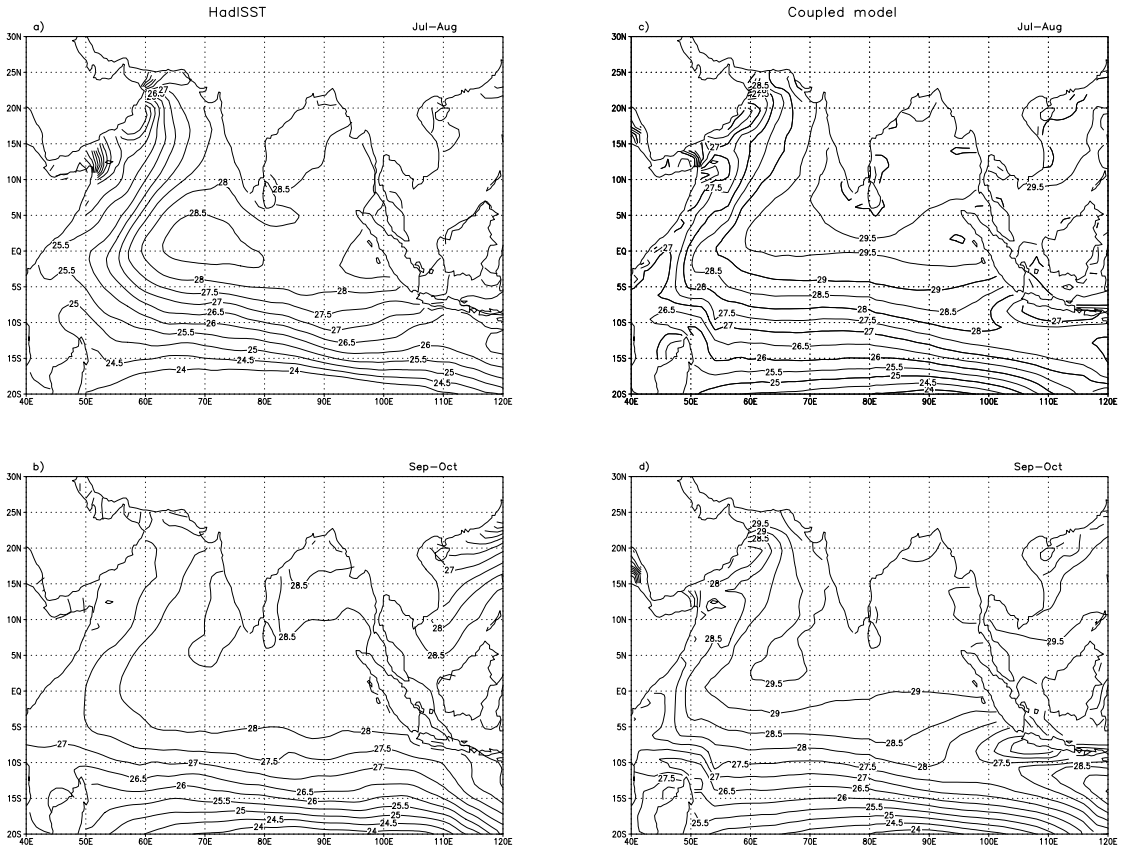

Fig. 1. Climatology of SST (deg C) averaged in July-August and in September-October for the HadISST dataset (panels a and b, respectively), and for the coupled model results (panels c and d, respectively). The contour interval is 0.5°C.

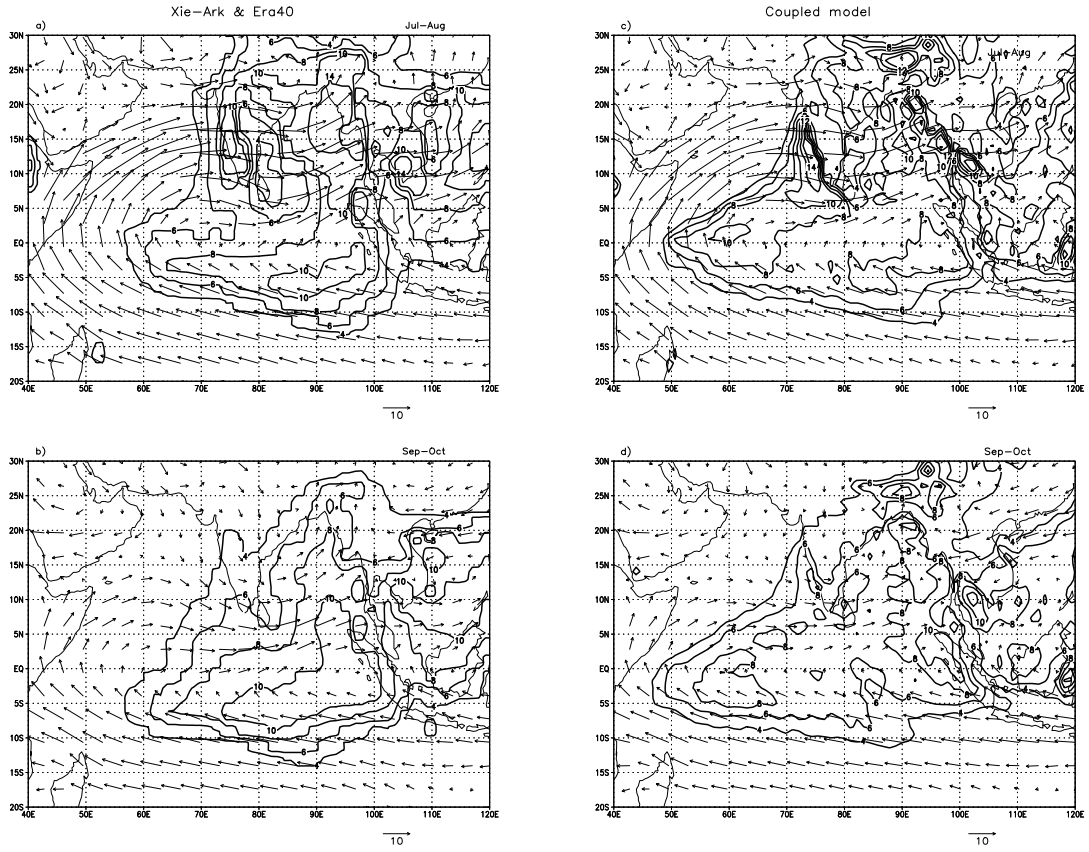

Fig. 2. Climatology of total precipitation (mm/day, contour lines) and of wind (m/sec, vectors) at 850 mb averaged in July-August and September-October for the CMAP dataset combined with ERA40 winds (panels a and b, respectively) and for the coupled model results (panels c and d, respectively). Contour intervals are 4,6,8,10 and 14 mm/day.

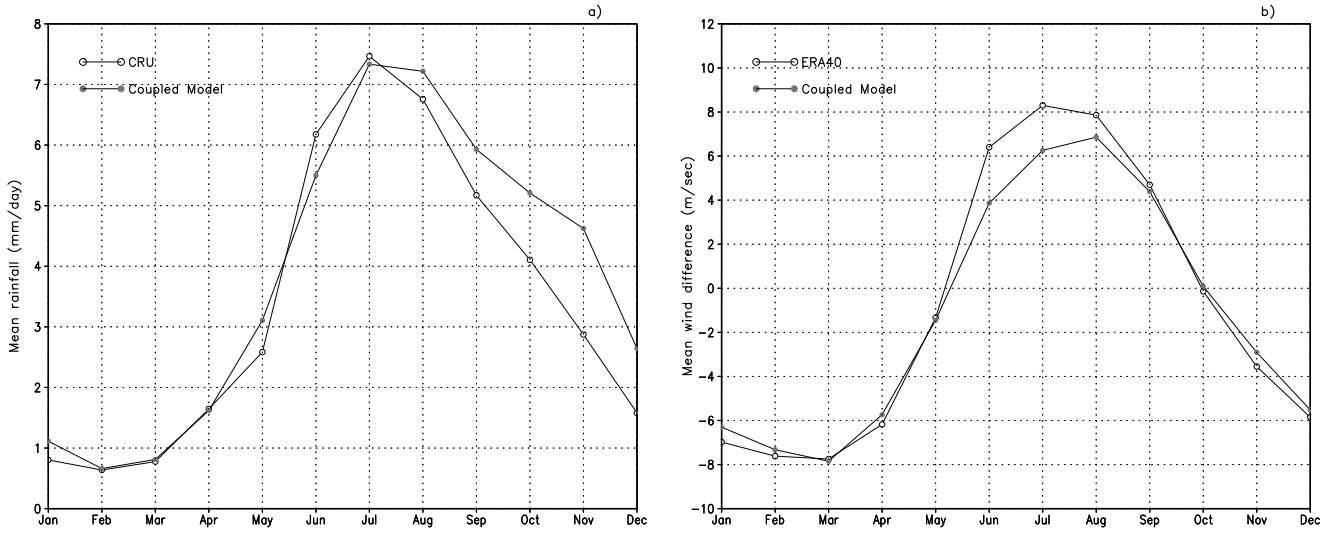

Fig. 3. Annual cycle of precipitation averaged over India (70-90°E, 5-30°N) for the observations (CRU dataset) and the coupled model results (panel a, lines with open and closed circles respectively) and annual cycle of IMI circulation index (see text for explanation) computed with zonal wind from the observations and from the coupled model results (panel b, lines with open and closed circles respectively).

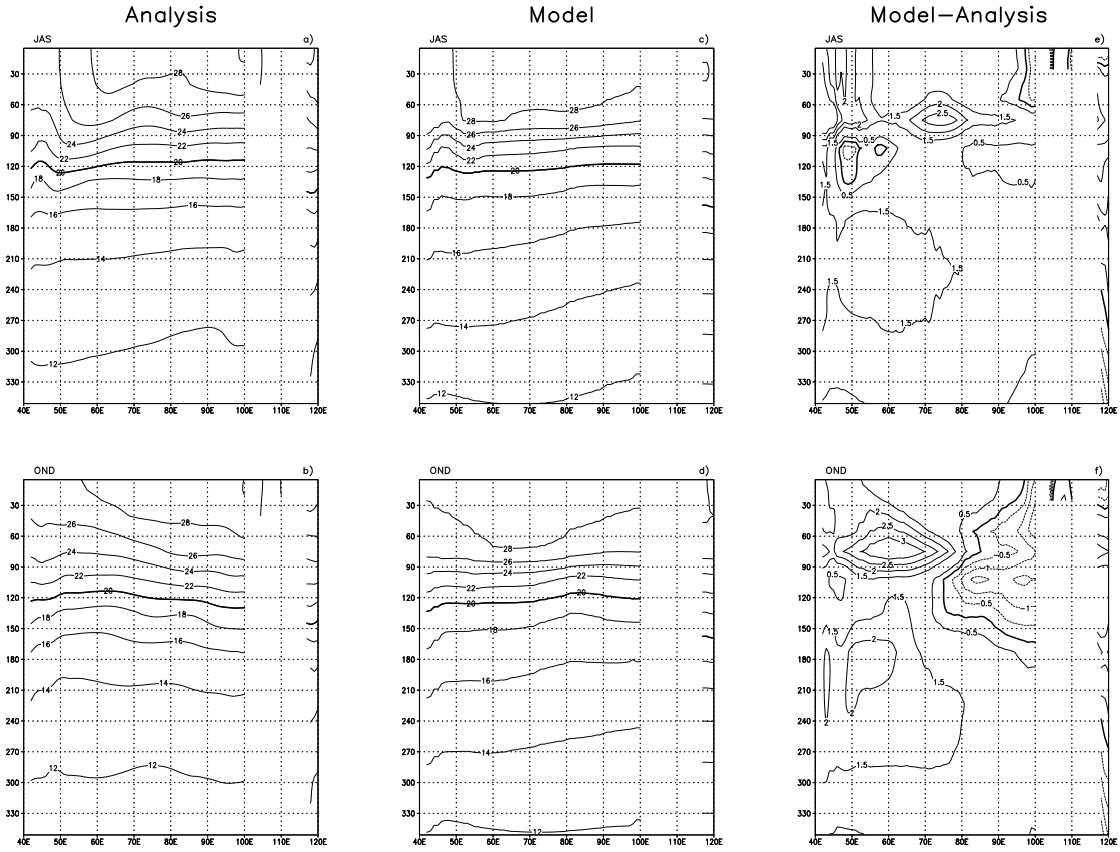

Fig. 4. Equatorial sections of temperatures in the Tropical Indian Ocean averaged in JAS and OND for the analysis (panels a and b) and for the coupled model experiment (panels c and d). Contour interval is 2°, and the thicker line correspond to the 20° isotherm. Panels e and f show the differences of the model minus the analysis temperatures for the same seasons. Contour intervals are -2 -1.5 -1. -0.5 0 0.5 1 1.5 2 2.5 3, and the thicker line correspond to the 0 contour line.

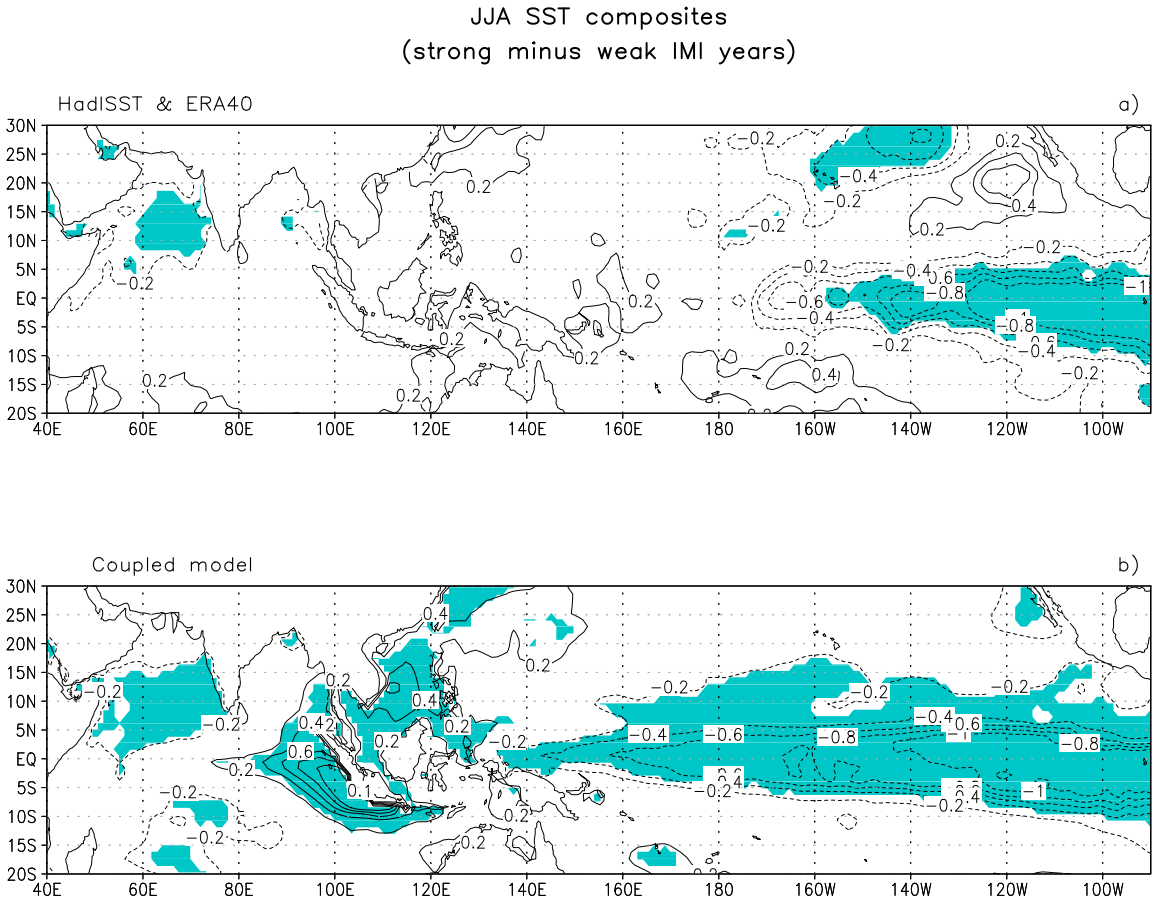

Fig. 5. Composites of JJA SST anomalies (C deg) for the observations (panel a) and for the coupled model results (panel b). Strong minus weak monsoon years according to IMI index are chosen. Values shaded are significant at 95%.

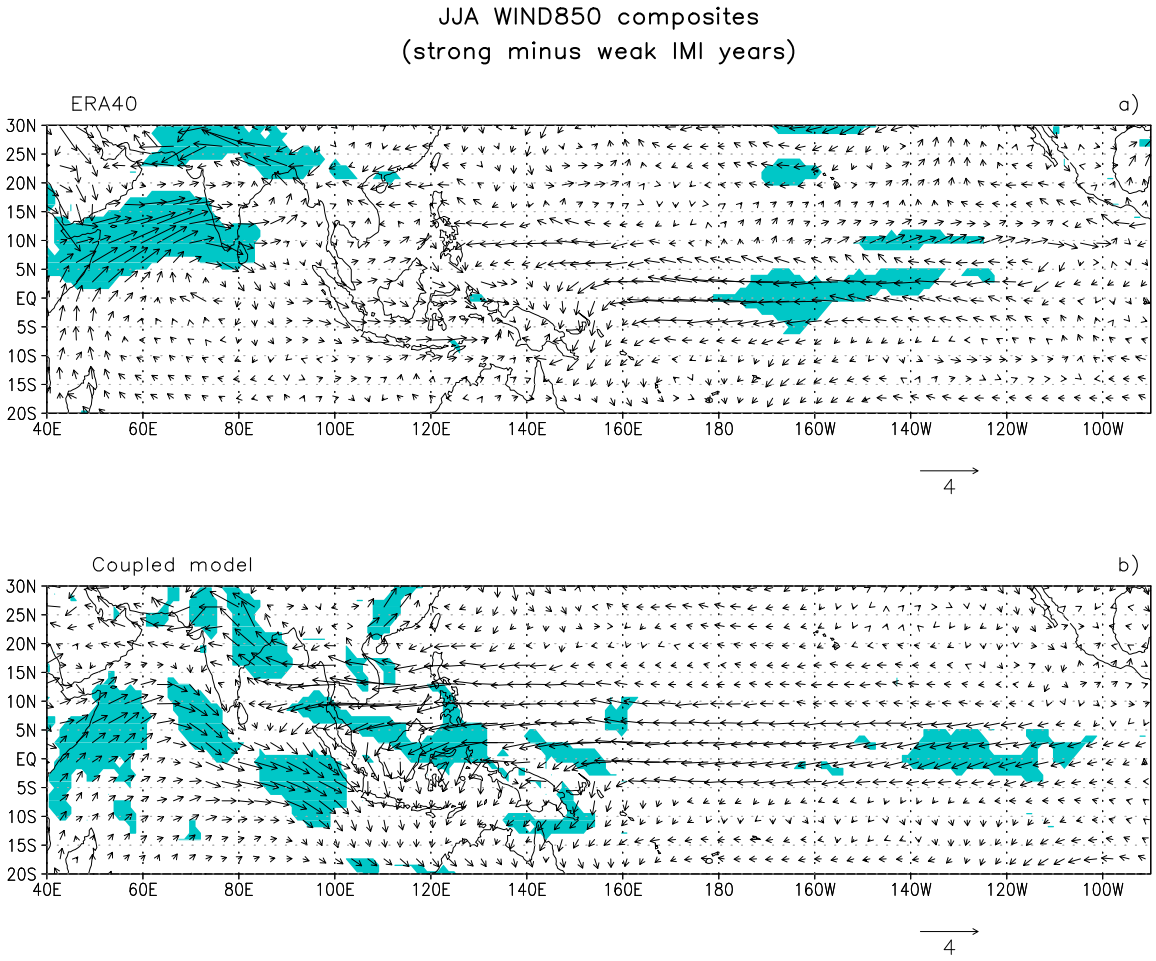

Fig. 6. Composites of JJA wind anomalies at 850 mb (m/sec) for the observations (panel a) and for the coupled model results (panel b). Strong minus weak monsoon years according to IMI index are chosen. Values shaded are significant at 95%.

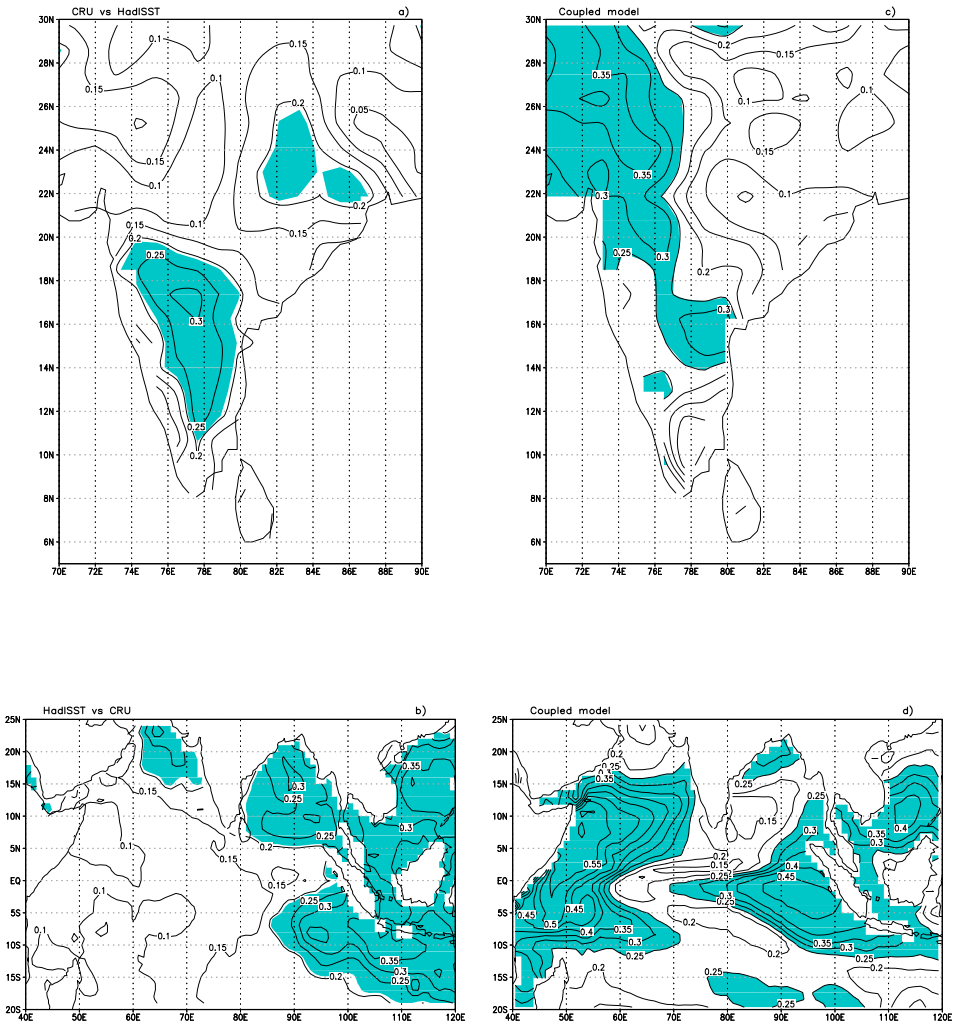

Fig. 7. Ratio of the ”forced manifold” variance to the total variance for summer precipitation in India (70-90°E, 5-30°N) (upper panels) and for the the summer SST anomalies in the Tropical Indian Ocean (40-120°E, 20°S-25°N) (bottom panels) for the observations (CRU vs HadISST, panels a and b, respectively) and for the coupled model results (panels c and d, respectively). Values shaded are higher than 0.2. All the values shown are significant at 95%.

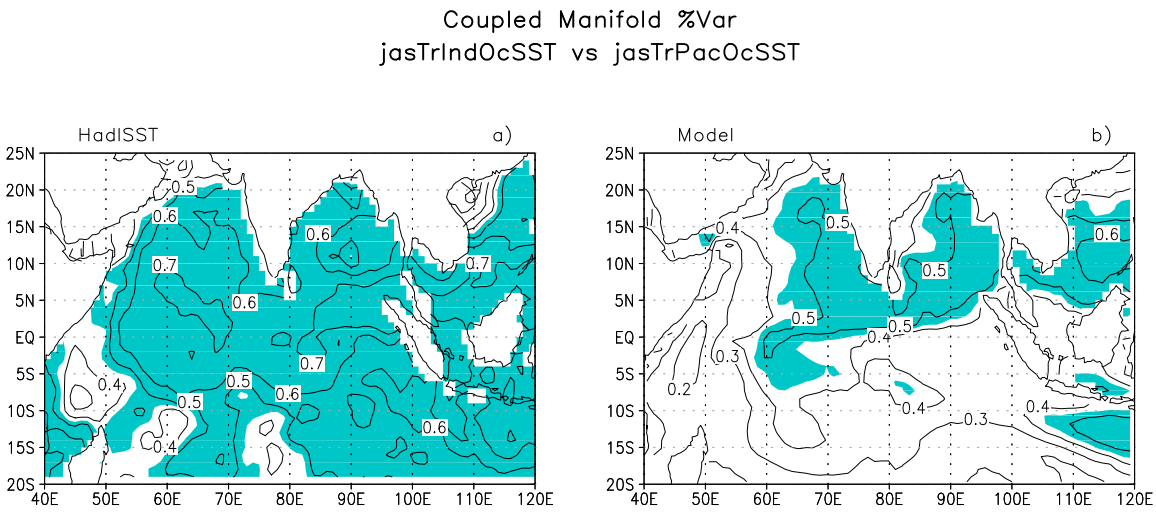

Fig. 8. Ratio of the ”forced manifold” variance to the total variance for summer SST anomalies in the Tropical Indian Ocean (40-120°E, 20°S-25°N) linked to SST anomalies in the Tropical Pacific Ocean (120°E-90°W, 30°S-30°N) for the observations (HadISST dataset, panel a) and for the coupled model results (panel b). Values shaded are higher than 0.4. Only values significant at 95% are shown.

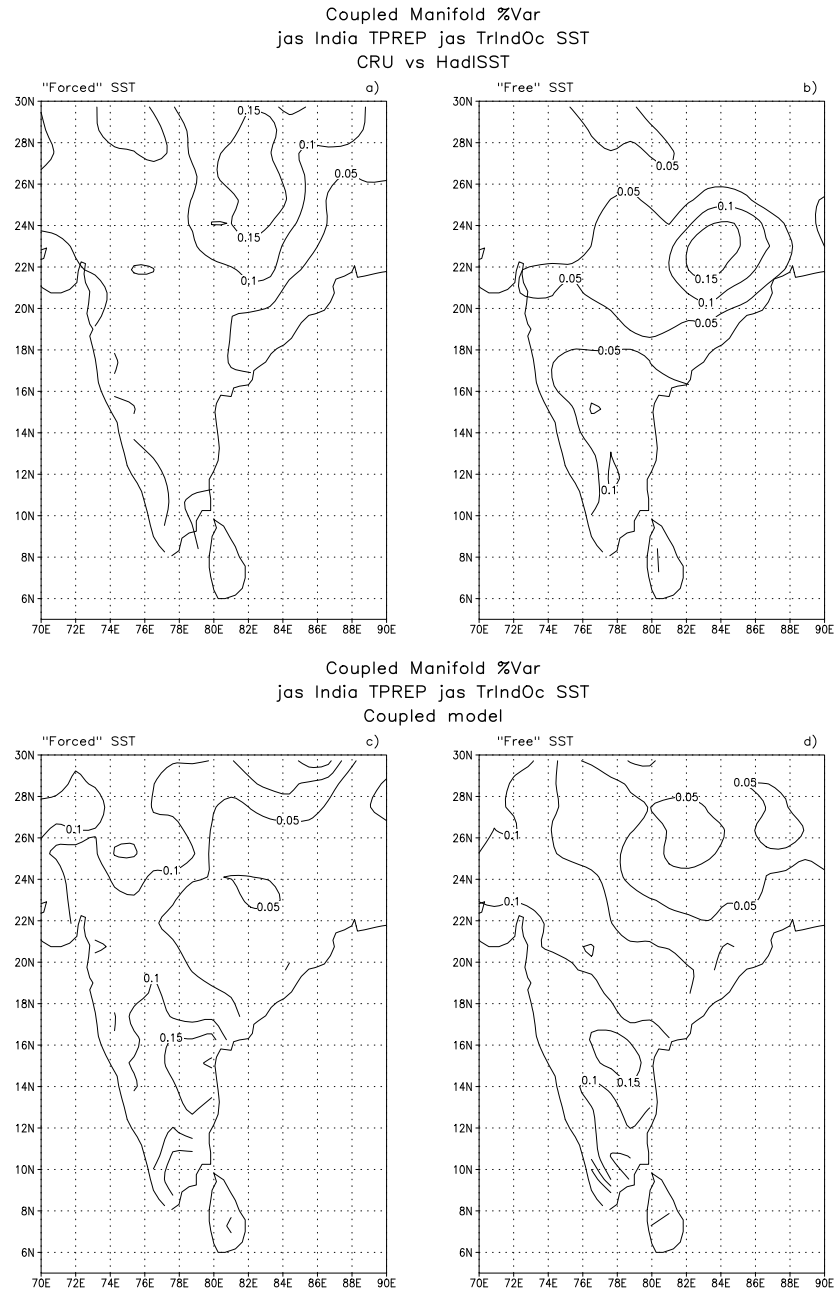

Fig. 9. Ratio of the ”forced manifold” variance to the total variance of summer precipitation in India with ”forced” and ”free” SST anomalies in the Tropical Indian Ocean for the observations (panels a and b, respectively) and for the coupled model results (panels c and d, respectively). ”Forced” and ”free” are referred to the influence from the Tropical Pacific Ocean. Only the values significant at 95% are shown.

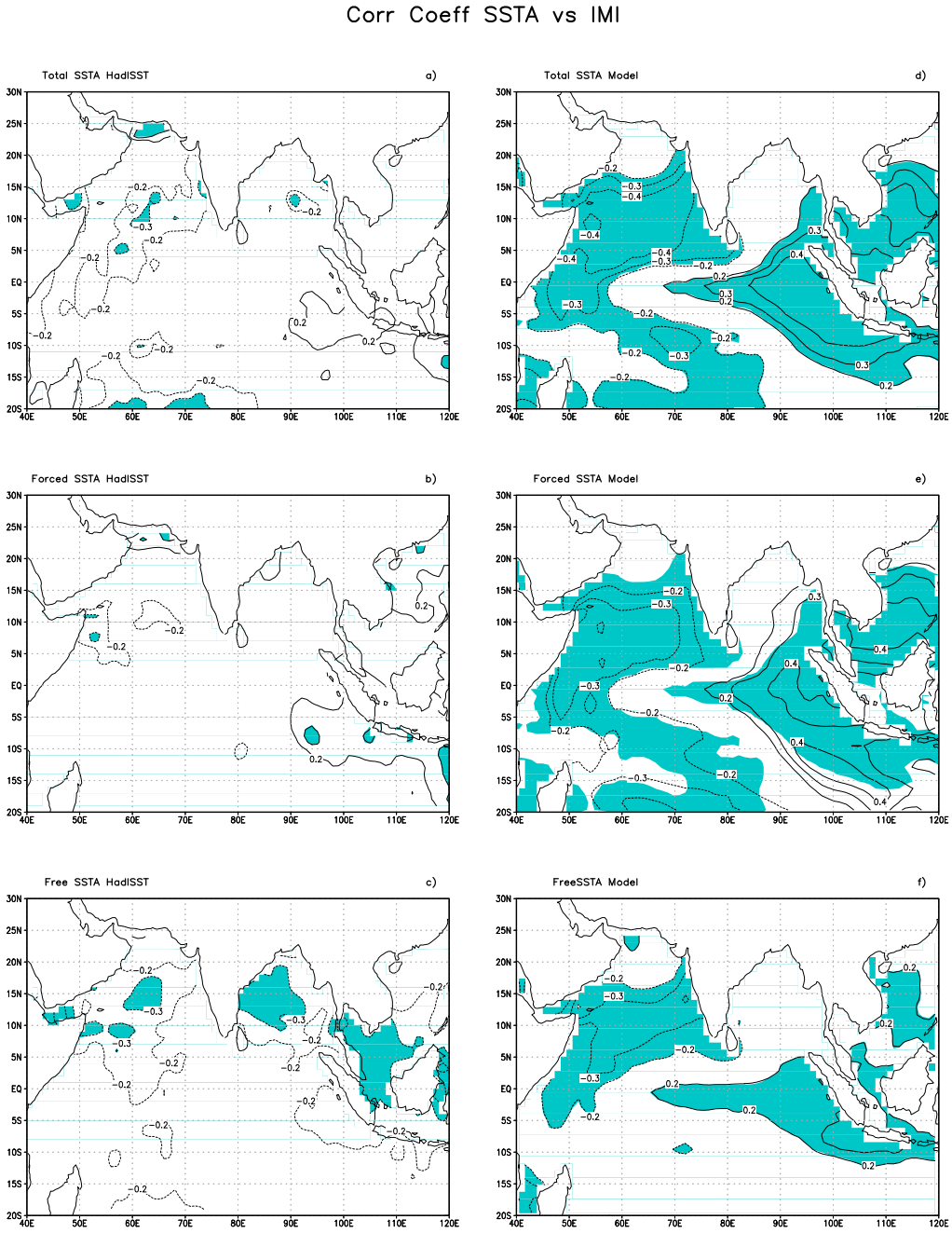

Fig. 10. Correlation coefficients between IMI and total, ”forced” and ”free” SST anomalies in the TIO for the HadISST dataset (panels a, b and c, respectively) and for the coupled model results (panels d, e and f, respectively). Values shaded are significant at 95%.

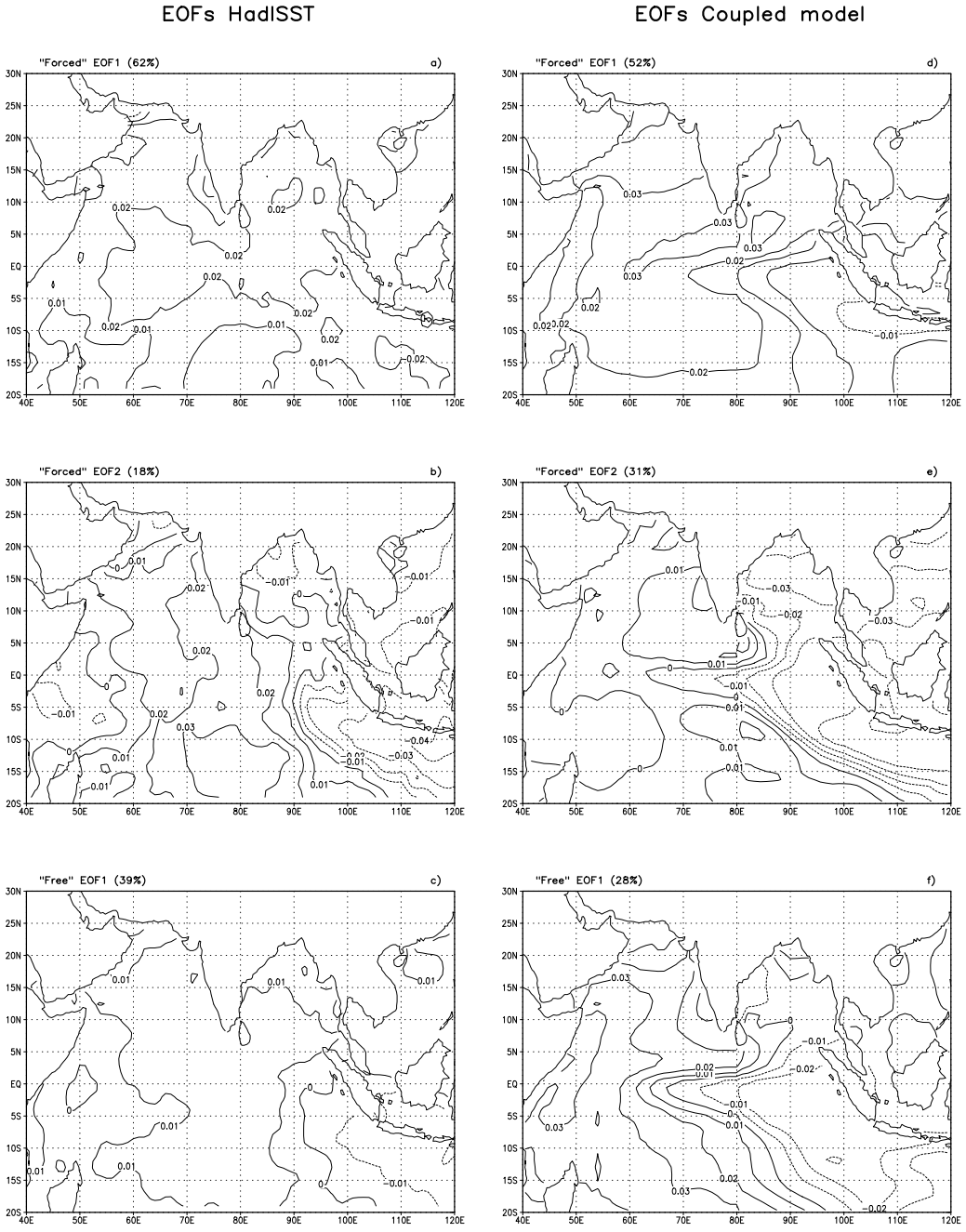

Fig. 11. First and second EOFs of the ”forced” Tropical Indian Ocean SST anomalies for the HadISST dataset (panels a and b, respectively) and for the coupled model results (panels d and e). First EOF of the ”free” Tropical Indian Ocean SST anomalies in the HadISST dataset (panel c) and in the coupled model results (panel f). ”Forced” and ”free” refers to the influence from the Tropical Pacific Ocean.